remote sensing

Article

Climatological Drought Monitoring in Switzerland Using EUMETSAT SAF Satellite Data

Annkatrin Rassl [1], Dominik Michel [2], Martin Hirschi [2], Anke Duguay-Tetzlaff [1,*] and Sonia I. Seneviratne [2]

[1] Federal Office of Meteorology and Climatology MeteoSwiss, 8058 Zürich, Switzerland
[2] Institute for Atmospheric and Climate Science, ETH Zürich, 8092 Zürich, Switzerland
* Correspondence: anke.duguay-tetzlaff@meteoswiss.ch

Abstract: Climatological drought monitoring in Switzerland relies heavily on station-based precipitation and temperature data. Due to the high spatial variability and complexity of droughts, it is important to complement station-based drought indices with gridded information and to couple multiple drought indicators within the monitoring system. Here, long-term satellite-based drought parameters from the EUMETSAT SAF network are analyzed in terms of dry anomalies within their climatology's, namely ASCAT soil water index (SWI), CM SAF land surface temperature (LST), complemented with NOAA vegetation data, and LSA SAF Meteosat evapotranspiration data. The upcoming EUMETSAT SAF climate data records on land surface temperature and evapotranspiration will cover for the first time the WMO climatological 30-year reference period. This study is the first study investigating the potential of those long-term data records for climate monitoring of droughts in Europe. The satellite datasets are compared with the standardized precipitation index (SPI), soil moisture observations from the SwissSMEX measurement network, with a modelled soil moisture index (SMI) based on observations, and with evapotranspiration measurements, focusing on the temporal dynamics of the anomalies. For vegetation and surface temperature, the dry years of 2003, 2015, and 2018 are clearly visible in the satellite data. CM SAF LSTs show strong anomalies at the beginning of the drought period. The comparison of in situ and modelled soil moisture and evapotranspiration measurements with the satellite parameters shows strong agreement in terms of anomalies. The SWI indicates high anomaly correlations of 0.56 to 0.83 with measurements and 0.63 to 0.76 with the SMI at grassland sites. The Meteosat evapotranspiration data strongly agree with the measurements, with anomaly correlations of 0.63 and 0.67 for potential and actual evapotranspiration, respectively. Due to the prevailing humid climate conditions at the considered sites, evapotranspiration anomalies during the investigated dry periods were mostly positive and thus not water limited, but were also a driver for soil moisture drought. The results indicate that EUMETSAT SAF satellite data can well complement the station-based drought monitoring in Switzerland with spatial information.

Keywords: spatial drought monitoring; severe drought events; drought climatology

check for updates

Citation: Rassl, A.; Michel, D.; Hirschi, M.; Duguay-Tetzlaff, A.; Seneviratne, S.I. Climatological Drought Monitoring in Switzerland Using EUMETSAT SAF Satellite Data. *Remote Sens.* **2022**, *14*, 5961. https://doi.org/10.3390/rs14235961

Academic Editor: Xianjun Hao

Received: 6 September 2022
Accepted: 17 November 2022
Published: 25 November 2022

1. Introduction

Droughts can have dramatic consequences for forestry, agriculture, ecosystems, and many more areas [1,2], and have long-term socio-economic impacts [2]. Central Europe and Switzerland have been affected by several major drought events in the last decades. The years 2003, 2015, and 2018 were exceptionally dry [3–5] and highlighted Europe's vulnerability to this natural hazard, alerting the public and governments to the need for drought mitigation measures [6] and effective drought monitoring. According to the Swiss Climate Change Scenarios CH2018 [7], there is a tendency towards even longer dry spells and increasing summer drying in Switzerland with increasing global warming in the coming decades, a tendency also confirmed for agricultural and ecological droughts in the latest assessment of the Intergovernmental Panel on Climate Change (IPCC) for Central and Western Europe [8]. To be able to evaluate the long-term evolution of drought events in Switzerland, climatological drought monitoring is fundamental. It creates the basis for effective adaptation and mitigation measures and helps to reduce the negative impacts of drought.

It is widely accepted that drought is a complex and multi-scalar phenomenon. It affects different parts of natural systems at different temporal time scales, which results in a diverse set of possible drought types [8–10] and impacts [11]. Drought monitoring systems should thus be integrated, coupling multiple variables and indices to fully characterize drought and its potential impacts [2,11–14]. While precipitation is the lead factor controlling the formation and persistence of drought [15], soil moisture, land surface temperature (LST), vegetation health, and evapotranspiration are likewise important variables to consider when aiming for an impact-based and holistic view on drought. In the IPCC 6th assessment report, separate assessments were for instance provided for changes in agricultural and ecological droughts (lack of soil moisture, sometimes amplified by increased atmospheric evaporative demand), hydrological droughts (low discharge and groundwater storage, low lake and reservoir levels), and meteorological droughts (lack of precipitation) [8]. Soil moisture is defined as the water stored in the unsaturated soil zone (e.g., [16]). It is the main source of water for vegetation, and thus a key variable affecting drought impacts on ecosystems and agriculture [17]. It is also a fundamental component for effective drought monitoring [18,19], as soil water deficit can be observed relatively early compared to other drought impacts such as plant water stress or reduced biomass [20]. In addition, the LST provides valuable information on surface moisture and potential drought conditions [21], as a dry surface heats up more strongly during the day when the air temperature is high. Drought stress during the growing season causes many plants to change the coloring of their leaves. This effect helps to evaluate the impacts of drought on natural vegetation [4,20]. Studies show that information on vegetation, especially when coupled to other drought indicators, provides a powerful tool for monitoring drought events [22–27]. Finally, evapotranspiration is also an important variable for drought monitoring [28]. Evapotranspiration is the flux of water from a surface area to the atmosphere. It comprises both plant transpiration and evaporation from moist surfaces. As the air temperature rises, evapotranspiration increases (depending on the local water availability) and soil moisture reduces. However, of note is the fact that despite rising air temperatures, evapotranspiration may also decrease at times. This is often due to exhausted water reserves in the soil [29].

Traditionally, climatological drought monitoring has been heavily based on precipitation and temperature station data. These variables tend to substantially vary between locations. In Switzerland, most measurement stations' data come from areas located in Northern Switzerland (Figure 1) within the temperate climatic zone. Due to the high spatial variability and complexity of drought events in Switzerland, it is important to complement the station-based drought indices with gridded information, as provided by satellite-based drought indices. In recent years, Earth observation satellites have been widely used to monitor drought and to assess its impacts [18,30]. Satellite-based data help to reduce the limitations of in situ drought monitoring by providing a large number of drought-relevant parameters in high spatial and temporal resolution for the whole of the Earth. In particular, it is possible to extensively and continually observe the surface dryness or moisture, vegetation, and the thermal states related with drought [24]. Satellites thus also provide information on the impacts of drought on soil and vegetation. Moreover, satellite drought measurements allow for scaling of the often costly and labor-intensive in situ measurements of soil moisture or other drought parameters to a larger regional area.

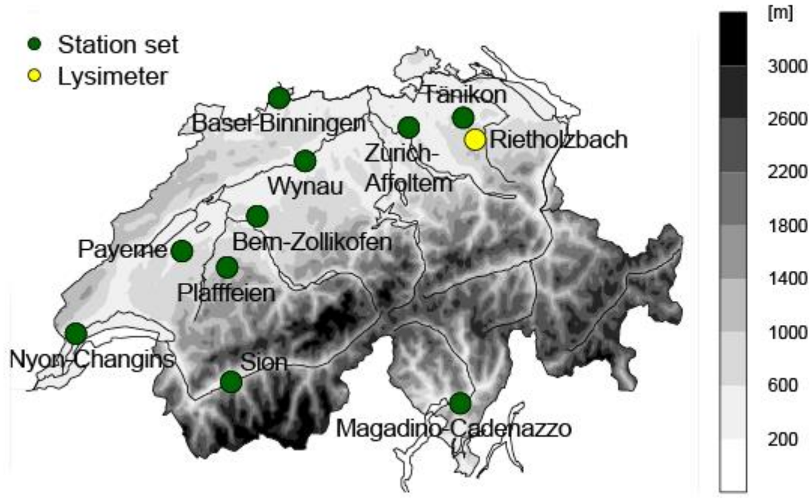

Figure 1. Location of the considered grassland station set (**green**) and the lysimeter station in Rietholzbach (**yellow**).

Satellite-based drought indicators generally used in drought monitoring systems are the vegetation heat index (VHI) [31] and the soil water index (SWI) [32]. The SWI is derived from satellite-based surface soil moisture data retrieved from radar measurements. The VHI [31] is a widely used remote-sensing drought index calculated as the weighted sum of the vegetation condition index (VCI) and the thermal condition index (TCI). The VCI and TCI compare the observed normalized vegetation index (NDVI) or land surface temperatures (LSTs) to the minimum and maximum values observed for the pixel over the entire climatological period. The standardized precipitation index (SPI; [9]) is based on precipitation records and generally shows the standardized deviation of the mean climatic precipitation in the long-term comparison. The index values directly indicate a probability of precipitation that can be calculated at any number of timescales.

In this study, we analyze the potential of EUMETSAT Satellite Application Facility (SAF) data for climatological drought monitoring in Switzerland. The EUMETSAT SAFs provide a unique set of satellite-based parameters for climatological drought monitoring. Soil moisture, land surface temperature, and evapotranspiration data are produced with a high spatial and temporal resolution both in near real-time and as long-term climate data records [33–36]. Those data have been analyzed extensively in the context of heat and drought (e.g., [37–39]). However, comprehensive analysis to highlight its potential for operational climatological drought monitoring is still missing.

The upcoming EUMETSAT SAF climate data records on land surface temperature and evapotranspiration will cover the full WMO climatological 30-year reference period of 1991–2020. Hence, those unique climate data are of high interest for climate monitoring. For the first time, we analyzed the potential of the EUMETSAT Satellite Application Facility (SAF) data in the context of climate monitoring to complement the existing station- and mainly temperature- and precipitation-based climatological drought data in Switzerland with spatial information of multiple drought-relevant variables.

The aim of this study is to compare long-term satellite data with station-based observations and drought indices in terms of known dry anomalies within their climatologies. In doing so, the potential of an integrated and spatial drought monitoring system for Switzerland can be assessed.

A detailed validation of the considered datasets has already been thoroughly carried out in other studies (see citations in the respective data sections below).

2. Materials and Methods

The study considers long-term satellite-based climate data from the EUMETSAT Satellite Application Facility (SAF) network. These spatial data are transferred to climatological drought indices and compared to station-based drought indices referred to as reference datasets. The focus lies on the challenging region of Switzerland and ten different grassland sites mainly located in the northwestern part of Switzerland (Figure 1), which have been heavily affected by drought events in recent years [4,40]. The station set also includes sites in complex topography (Sion) and in the southern part of Switzerland (Cadenazzo), and the considered sites all include soil moisture measurements [41] (see Section 2.2). For the evapotranspiration analysis, the grassland site in Rietholzbach is included due to its continuous and high-quality data coverage of lysimeter measurements [42,43]. For most drought indicators, the longest available time period is considered and the dry years of 2003, 2015, and 2018 are included in the analysis where possible (see Table 1).

Table 1. Analyzed time periods for the considered drought indicators.

Drought Indicator	Time Period
SPI	2003, 2015, 2018
VHI	2000–2019
VCI	2000–2019
TCI	2000–2019
LST	2010–2019
ASCAT SWI	2011–2018
SMI	2011–2018
SwissSMEX soil moisture	2011–2018
LSA SAF ET	2006–2015
LSA SAF ETP	2006–2015
Lysimeter ET	2000–2020

2.1. Satellite Data

The main datasets analyzed in this study are satellite data from the EUMETSAT Satellite Application Facility (SAF) including Advanced Scatterometer (ASCAT) soil water, Meteosat land surface temperature, which is complemented with NOAA AVHRR vegetation data, and Meteosat evapotranspiration. The considered datasets are operational and are—or will soon be—freely available for climate services. Some of the datasets are integrated in the EUMETSAT Drought & Vegetation Data Cube (https://training.eumetsat.int/course/view.php?id=399 accessed on 22 November 2022), which greatly facilitates data access and assimilation. From the variety of SAF data, homogeneous climate data records were selected that also cover long time periods of at least eight years.

The study considers a precursor version of the upcoming Hydro (H) SAF ASCAT disaggregated surface soil moisture v2 data further translated into the soil water index (SWI) [32]. The H SAF ASCAT surface soil moisture (SSM) is derived from radar backscattering coefficients measured by ASCAT on-board the series of MetOp satellites with a quasi-daily global coverage and 25 km spatial sampling [33,44]. The ASCAT SWI translates the measured soil moisture content of the upper few centimeters of the soil into moisture content within the underlying soil profile. The SWI algorithm uses a two-layer water balance model [45] to describe the relationship between surface soil moisture and profile soil moisture as a function of time [33]. The SWI is provided for different T-values [46], which determine how strongly SSM observations from the past influence the current SWI. As the water content of the reservoir is solely controlled by the past moisture conditions in the assumed model, T-values can be directly translated into soil depth for similar soils [33]. For this study, a T-value of 10 is selected, which refers to a soil depth down to about 50 cm for column-integrated soil moisture ([47]. The ASCAT SWI investigated here is a new version, which includes, in addition to improved vegetation correction parameters, a detrending for ASCAT SSM by 12.5 km spatial sampling and, based on those data, a directional SWI downscaling to 500 m. The ASCAT SWI test data were provided by the Vienna University of Technology (TU Wien) and are considered for the period of 2011 to 2018 (see Table 1) in a regular 0.005 lat/lon grid.

Tong et al. [48] validated the ASCAT SWI data in 213 catchments in Austria for the period of 2000–2014. They found that including the ASCAT SWI data in the calibration of an HBV (Hydrologiska Byråns Vattenbalansavdelning)-type hydrologic model could mainly improve the soil moisture simulations. The median soil moisture correlation between ASCAT SWI and hydrologic model outputs was 0.4 to 0.52 and was thus much higher than the median of 0.26 found by [49] using the coarser European Remote Sensing (ERS) scatterometer data in model calibration.

Note that soil moisture retrieval with satellites in mountainous regions is especially complex due to various error sources on the radar backscatter such as snow and ice cover as well as reduced sensitivity due to rocks [32]. Thus, the satellite-based dataset for Sion (Figure 1) is subject to a large number of missing values (38%; see also Table 2).

Table 2. Percentage of missing data for soil moisture datasets (analyzed period: 2011–2018, April–October).

Station	SWI	SMI	SwissSMEX
BAS	0.6	0	63.1
BER	1.5	0	2.6
CAD/MAG	8.8	0	9
CHN/CGI	1.6	0	48.8
PAY	0.9	0	0
PLA/PLF	9.9	0	0.6
REC/REH	0.6	0	0.4
SIO	38	0	32.4
TAE	0.9	0	1.9
WYN	0.9	0	8.1

In addition to the ASCAT SWI, we calculate the vegetation health index (VHI) based on the land surface temperatures of the Satellite Application Facility on Climate Monitoring (CM SAF; precursor version of the upcoming CM SAF Meteosat Land Surface Temperature Climate Data Record v2) and the vegetation condition index of the National Oceanic and Atmospheric Administration (NOAA). LST meets the 2.0 K target precision and 1.3 K target accuracy when compared to more than 50,000 LST measurements from the LSA SAF in situ sites which include various atmospheric conditions [34,50]. The comparison of the LST data with skin temperatures of the European Centre for Medium-Range Weather Forecasts (ECMWF) and LST of the Moderate-resolution Imaging Spectroradiometer (MODIS) fulfils the 0.8 K decadal stability requirement [34]. The LST data were atmospherically corrected through the implicit use of radiative transfer models [44]. Regular gridded CM SAF LSTs are translated into the TCI by assembling 10:00 UTC clear sky LST observations into 7-day TCI composites. We calculate the VHI from weekly NOAA VCI and transformed CM SAF LSTs (represented as TCI) with a weight of 0.5 following standard procedures [51]. The VHI generated in this study has a 7-day temporal resolution on a regular 5 km lat/lon grid. LST data are available for the time period of 2010 to 2019, and the VHI, VCI, and TCI data are available for the time period of 2000 to 2019 (see Table 1). In terms of VHI and VCI, note their usability during the growing season only. From November to March with almost no green vegetation, these indices can hardly provide an indication of drought.

This study further considers two different evapotranspiration datasets from the Land Surface Analysis (LSA) SAF, namely the Meteosat Second Generation (MSG) reference evapotranspiration (ETP, LSA-303 v1 labelled METREF) and the MSG actual evapotranspiration (ET, LSA-301 v1 labelled MET). The two datasets are derived from an MSG SEVIRI instrument with an image repeat cycle of 30 min and a 3 km pixel resolution at nadir. MSG views most parts of Europe and Africa. The LSA-303 ETP is a homogeneous climate data record at daily resolution considered from 2006 to 2015 (see Table 1) and corresponds to the evapotranspiration rate from a hypothetical extensive well-watered field covered with 12 cm-high green grass with an albedo of 0.23 [35]. Moreover, the considered ETP dataset is primarily estimated from the LSA SAF Daily Downward Surface Shortwave Flux dataset. It only presents a slight dependency on ECMWF near the surface air temperature [35]. Hence, the down-welling short-wave radiation is the main driver for the LSA SAF ETo. Reference [35] validated the considered ETo dataset by comparing it with measurements of grassland sites in Germany (Falkenberg and Rollesbroich) and the the Netherlands (Cabauw), among others. The validated sites have similar climatic characteristics compared to the station set of the present study. Validation results show that LSA SAF ETo data agree well with in situ measurements. Root mean square differences between LSA SAF ETo and the observations offered values of 0.7 mm/day, 0.6 mm/day, and 0.4 mm/day, respectively.

The LSA-301 ET accounts for the actual water vapor flux between the earth land surface and the atmosphere including evaporation from soil, water and canopy as well as transpiration from plants. The ET is estimated from the adapted HTESSEL land surface model using satellite-based data (LSA SAF shortwave and long-wave downwelling radiation, albedo, land surface temperature) and various other satellite-based ancillary data (e.g., vegetation and snow) as model input [36]. The LSA-301 ET dataset is retrieved from the LSA SAF website (https://landsaf.ipma.pt/ accessed on 22 November 2022) for the period of 2006 to 2015 (see Table 1). Hourly LSA-301 ET data were aggregated into daily composites. The in situ validation of [36] shows that the considered ET dataset is in good agreement with the observations, considering the time period of March 2007 to December 2011 and a large number of measurement sites across Europe and Africa with different climate and vegetation types. The correlation between LSA SAF ET and observations at grassland sites in Europe, for instance, is over 0.7 and the root mean square error (RMSE) is below 0.1 mm/h.

The two LSA SAF evapotranspiration datasets were re-gridded into regular lat/lon grids covering Switzerland.

2.2. In-Situ Measurements

This study compares the satellite-based data with different reference datasets, namely with observations of the nationwide soil moisture monitoring program Swiss-SMEX (Swiss Soil Moisture Experiment; [41]), with in situ evapotranspiration from a weighable lysimeter at the Rietholzbach site [42,43] and with the standardized precipitation index (SPI; [9]) calculated from rain gauge measurements.

The considered SwissSMEX data comprise soil moisture measurements in mm water column, integrated over the top 50 cm of the soil using the trapezoidal method (e.g., [52]). The used sensors are TDR (time domain reflectometry) TRIME PICO-64 (IMKO GmbH, Germany), and capacitance 10HS (Decagon, USA, retired) at soil depths of 5, 10, 30, and 50 cm, measuring the volumetric water content· Note that for some of the stations the amount of missing data is substantial (e.g., 63.1% at the site BAS) due to sensor failures at specific depths for prolonged time periods, which make it impossible to derive column-integrated soil moisture (Table 2).

The weighable lysimeter for measuring evapotranspiration at the site in Rietholzbach has a surface area of 3.14 m^2 and a depth of 2.50 m. The accuracy of the lysimeter mass change due to precipitation, evapotranspiration, and gravitational seepage corresponds to 0.03 mm. Seepage is recorded with a tipping bucket with an accuracy corresponding to 0.02 mm. The surface cover is grass, matching the surrounding area [42,53]. The lysimeter records from 1975–2007 are analyzed in [42], and those from 2009 to 2015 are described and compared to parallel eddy-covariance-based evapotranspiration measurements in [43].

The standardized precipitation index (SPI; [9]) is based on precipitation records from Swiss measurement stations. Here, the timescale of three months is considered. SPI has an intensity scale in which both positive and negative values are computed. They correlate directly to wet and dry conditions. According to [9], drought events are indicated when the SPI becomes continuously negative and reaches a value of -1 or less. SPI values of -1.0 to -1.49 are considered as moderately dry, SPI values of -1.5 to -1.99 are considered as severely dry and SPI values of -2.0 or less are considered as extremely dry. With precipitation as the only input, in turn, SPI does not account for other aspects of drought events. It lacks the impact of the temperature component [54] and the related excess of evapotranspiration, which is important to the overall water balance of a region, for the soil moisture conditions and vegetation health. This study considers the SPI for the dry years of 2003, 2015, and 2018 (see Table 1).

The soil moisture measurements are considered at ten different grassland sites for the period 2011 to 2018, and the lysimeter measurements are considered for the grassland site in Rietholzbach from 2000 to 2020 (see Figure 1 and Table 1). The SPI is also considered at the ten grassland sites and the calculation is based on the reference period of 1981–2010.

2.3. Model Simulations at the Sites

The model-based climatological soil moisture index (SMI) defines the soil moisture from daily values of precipitation and potential evapotranspiration for grasslands with average soil properties (13% field capacity, i.e., 52 mm plant-available water in the root zone with 40 cm root zone depth). More precisely, the underlying soil water model, based on the work of [55] and also referred to as the bucket model, considers measured precipitation as input and three outputs, namely run-off, drainage, and evapotranspiration. Evapotranspiration is calculated as a function of measured temperature, solar radiation, humidity, and wind speed. The model takes into account that above a certain amount of precipitation (27.4 mm/day), run-off occurs and that water drains from the soil as soon as the soil is saturated, i.e., when the soil moisture exceeds the field capacity. In addition, the model simulates that below a certain soil moisture level, vegetation releases less water than at an optimal water supply [55]. The SMI gives the soil moisture in volume percent and is considered for the defined station set and the time period of 2011 to 2018 (see Table 1).

2.4. Methods

To compare the satellite drought parameters with in situ observations and modelled data, the respective grassland locations (Figure 1) from the gridded datasets are extracted by taking the grid points closest to the station coordinates.

- For the SPI, daily data for the timescale of three months for 2003, 2015, and 2018 are calculated. By analyzing their temporal evolution (spatial average over the ten grassland locations), an indication of the precipitation conditions during these dry years can be obtained.
- For the vegetation and surface temperature datasets VHI, VCI, TCI and LST, first monthly means from weekly data are calculated, if there is at least one week of data. In the next step, the seasonal evolution (spatial average over the ten locations) of the long-term climatology is analyzed, i.e., the available data period excluding the dry years of 2003, 2015, and 2018. We analyzed the evolution of the years 2003, 2015, and 2018 in addition to this. In doing so, it is possible to see how the drought years are characterized in the different remote-sensing datasets.
- In terms of **soil moisture**, this study considers three datasets, namely the satellite-based SWI, SwissSMEX measurements, and the modelled SMI. Their seasonal evolution is analyzed according to the vegetation and surface temperature data, but instead of monthly absolute values, we consider daily anomalies averaged over the considered grassland sites (Figure 1). Anomalies are calculated with respect to the long-term mean based on the available data period (see Table 1) and excluding the dry years of 2015 and 2018. Using anomalies allows for a better comparison of the three datasets since their absolute soil moisture values are strongly dependent on local soil properties or underlying model assumptions and help identify how well the dry years are represented. For illustrative purposes, the time series of the long-term climatology are smoothed with a 14-day running mean window. Moreover, to compare the relationship between the satellite-based SWI and the two reference datasets (SwissSMEX measurements and modelled SMI), the Pearson correlation coefficient r is considered for every grassland site for the period of April to October of 2011 to 2018.

The correlation analysis is based on deseasonalized anomalies that are calculated as deviations from the mean seasonal cycle and applying a 3-day running mean on the resulting anomalies to fill single days of missing data (mainly present in the remote sensing dataset). The climatological mean for each day of the year was calculated by averaging daily values for all available years and smoothing it with an 11-day window.

- In terms of evapotranspiration, the study considers the two satellite-based datasets ET and ETP as well as the lysimeter measurements. The focus lies on the grassland site in Rietholzbach (Figure 1), where long-term and high-quality in situ evapotranspiration measurements are available. For the comparison analysis, we are especially interested in three questions. First, do the dry years of 2003, 2015, and 2018 stand out from average conditions in terms of evapotranspiration measurements? For this, the seasonal evolution of the long-term climatology from 2000 to 2020 (excluding the dry years of 2003, 2015, and 2018) are compared with the dry years of 2003, 2015, and 2018. Secondly, how do the satellite datasets agree with the measurements? For this, the satellite-based ET and ETP are compared with the measurement data in terms of the seasonal evolution of their long-term climatologies (2006 to 2014). Third, is there a larger difference between ET and ETP during dry conditions compared to average conditions? This would indicate a soil moisture-limited rather than an energy-limited system. We therefore compare ET and ETP in terms of the seasonal evolution of the spatially averaged climatology (2006 to 2014) and the dry year of 2015 at the considered station set. Note that for clarity, all evapotranspiration time series are smoothed with a 14-day running mean window. The mean bias, RMSE and Nash-Sutcliffe model efficiency coefficient (NSE) between in situ measured evapotranspiration and ET as well as ETP are calculated at the site in Rietholzbach based on the absolute values. In addition, r is considered for the hip between the respective deseasonalized anomalies.

3. Results

From the SPI analysis it can be seen that all three years, 2003, 2015, and 2018, indicate dry conditions with negative SPI values (Figure 2). In 2003, the spring season was already severely dry. Extremely dry conditions prevailed until autumn with a maximum severity of about −2 in mid-August. In 2015, spring and summer were normal to wet, and severe dry conditions did not set in before August, when the SPI abruptly dropped from 0 in July to almost −2 in August. The SPI remained negative throughout the remaining year. In 2018, dry conditions already set in from mid-April and prevailed throughout the year with a negative peak of below −2 in October. The maximum severity of drought in 2018 was thus similar to 2003, but about two months later.

The temporal evolution of the surface temperature and vegetation condition indicates strongly negative values during the dry years of 2003, 2015, and 2018 (Figure 3). The VHI (vegetation health and surface temperature; usable during growing season only, see Section 2.1) is well below the 95th percentile from May onwards for all three drought years, with the lowest values in August (Figure 3a). With respect to the magnitude of the dryness, 2018 is the most severe (except for the southern part of Switzerland; not shown), while 2003 and 2015 are slightly weaker in terms of vegetation health and surface temperature. 2018 also experienced a longer period of dry conditions, which lasted until November. 2003 and 2015 showed earlier recovery phases from September onwards. The longer duration of dry conditions in 2018 seems to be mainly due to the anomalously high surface temperatures that continue to stay high until the end of the year (shown as low TCI and high LST values; Figure 3c,d). In 2003 and 2015, surface temperatures had already returned to average in September. In 2015, surface temperatures rise again in November, not affecting the vegetation health however (no growing season). The VCI (usable during growing season only, see Section 2.1) shows a very similar temporal evolution during the three drought years with a rapid decline from June and particularly low values well below the 95th percentile in August (Figure 3b). The VCI returns to average conditions from September onwards. In 2003, the recovery is slightly earlier than in 2015 and 2018. Comparing the temporal sequence of vegetation health and surface temperature anomalies during the dry years shows that surface temperatures are anomalously high before vegetation health is affected (Figure 3b–d). For all drought years, the surface temperatures exceed the 95th percentile in June, while the vegetation response is delayed by about four weeks.

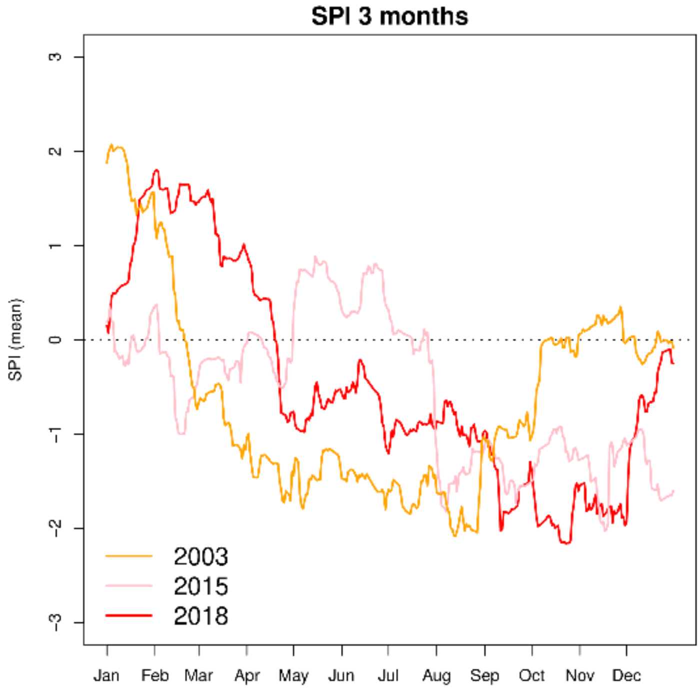

Figure 2. Seasonal evolution of daily standardized precipitation index (SPI, calculated for the three-month timescale), averaged over the considered grassland stations for the dry years of 2003, 2015, and 2018. SPI value of 0.99 to −0.99 = normal, −1.0 to −1.49 = moderately dry, −1.5 to −1.99 = severely dry, and −2.0 or less = extremely dry.

In addition, in terms of soil moisture, the dry years of 2015 and 2018 (no data for 2003) are well visible in the ASCAT satellite data (Figure 4). Comparing the satellite-based soil moisture data (Figure 4a) with the reference datasets (Figure 4b,c) shows that the soil moisture anomalies of the dry years 2015 and 2018 (with respect to the long-term mean) are represented in the measurements, and the modelled SMI and the gridded SWI are represented by showing a similar temporal evolution with pronounced phases of dryness. The anomalies of SMI and SWI are, however, underestimated compared to the SwissSMEX data. The 2018 event is characterized by an earlier onset of dry conditions (April) and a longer duration (November) compared to 2015, which is consistent with the SPI (see Figure 2). 2015 starts with comparable wet soils before there is a rapid decline in soil moisture from June (see also the SPI in Figure 2). This is clearly visible in all three datasets, despite some more variation in the SMI data (Figure 4c). With respect to the drought magnitude, 2018 is comparable to 2015 with values well below the 95th percentile during both years. In 2015, strongly negative anomalies are reached in July, which is consistently represented in the satellite data as well as in the reference data. Measurements, modelled SMI, (Figure 4b,c) and SPI (Figure 2) also indicate negative anomalies during November, which appear less pronounced in the satellite data (Figure 4a). In 2018, negative soil moisture anomalies happen especially throughout July and in October. The satellite and the modelled data replicate the autumn drought accordingly, while the summer dry period is shown as being slightly less severe in both datasets.

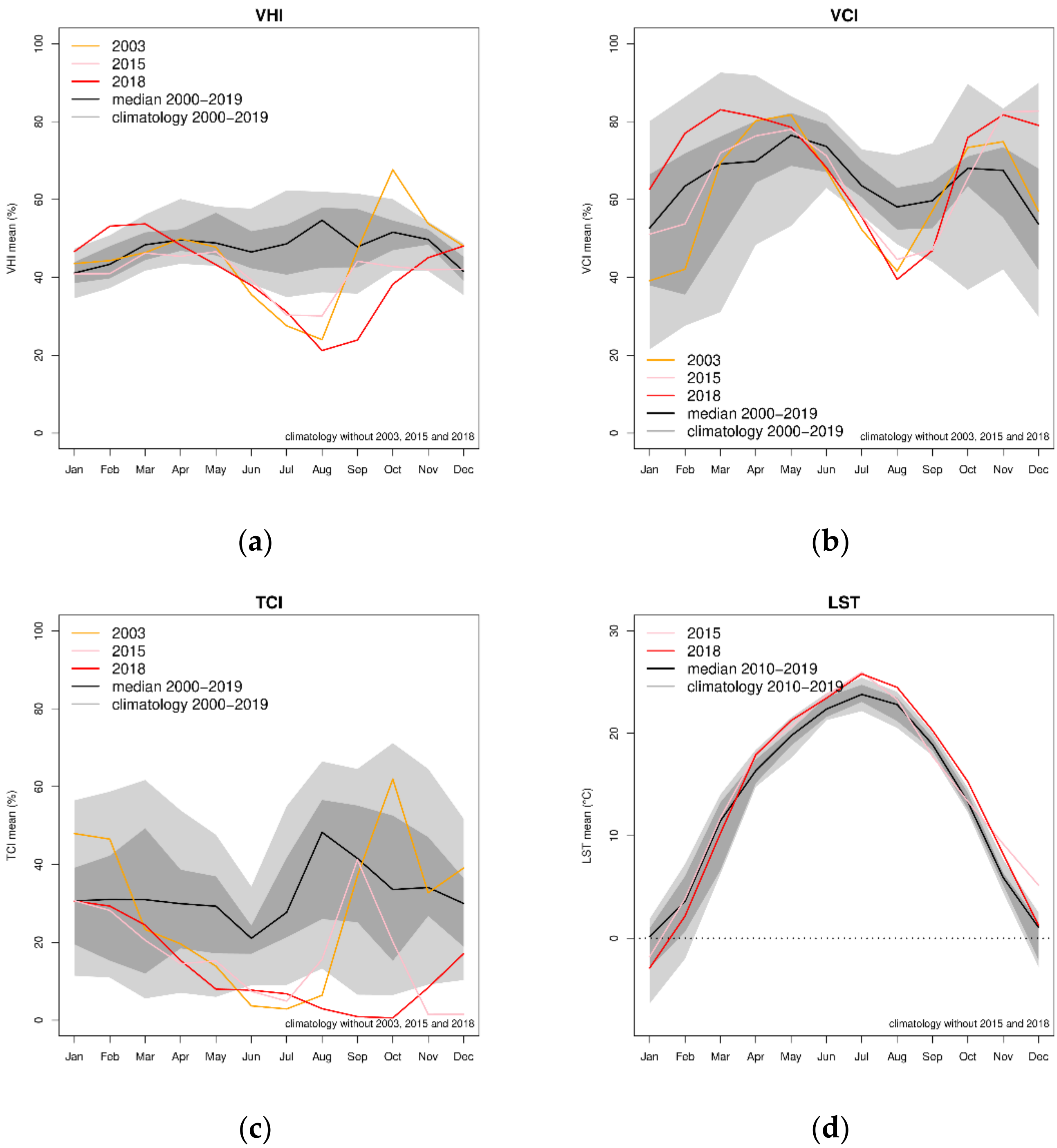

Figure 3. Seasonal evolution of monthly (**a**) vegetation health index (VHI), (**b**) vegetation condition index (VCI), (**c**) temperature condition index (TCI), and (**d**) land surface temperature (LST), averaged over the considered grassland stations. The background climatology in grey and black is based on the years of 2000 to 2019 (without the dry years 2003, 2015, and 2018) and 2010 to 2019 for LST (without the dry years of 2015 and 2018). The dark grey shading shows the 25–75% range of the respective background climatology; the light grey shading shows the 5–95% range. The evolution of the respective median as well as of the dry years is highlighted.

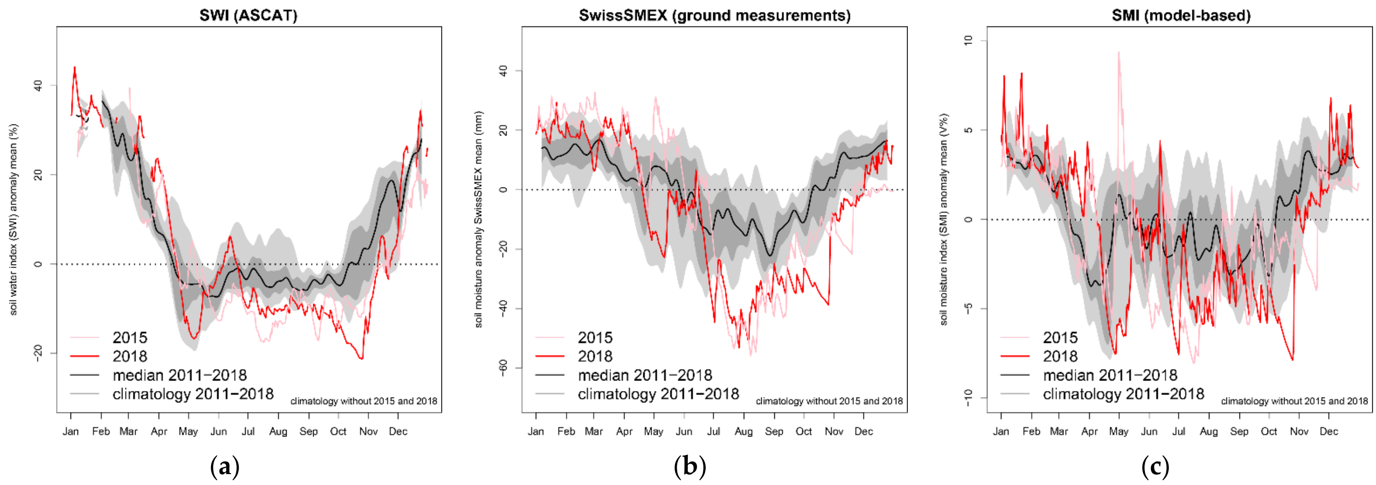

Figure 4. Seasonal evolution of daily soil moisture anomalies (anomalies w.r.t. the long-term mean), averaged over the considered grassland stations, for (**a**) the satellite-based ASCAT soil water index (SWI), (**b**) the station-based SwissSMEX soil moisture measurements, and (**c**) the modelled soil moisture index (SMI). The background climatology in grey and black is based on the years of 2011 to 2018 (without the dry years of 2015 and 2018). The dark grey shading shows the 25–75% range of the respective background climatology; the light grey shading shows the 5–95% range. The evolution of the respective median as well as of the covered dry years is highlighted.

The correlation of the satellite-based soil moisture data with the reference datasets is analyzed in terms of deseasonalized anomalies at the considered grassland stations (Figure 5). The satellite-based soil moisture dataset strongly correlates with the soil moisture measurements and modelled data: satellite-based anomalies indicate station-specific correlations of 0.56 up to 0.83 (except Sion) with the SwissSMEX anomalies (Figure 5a), and correlations of 0.63 to 0.76 with the model-based SMI anomalies (Figure 5b). Note that in Sion, the correlation between SWI and measurement data is much lower ($r = 0.26$) compared to the remaining sites. Sion is situated in a valley and surrounded by complex topography. Topographic complexity influences the correlation of ASCAT SWI and in situ data [56]. Soil moisture retrieval with satellites in mountainous regions is especially complex [32]. For the closest grid points to Sion, the satellite-based dataset is thus subject to substantial missing values (38%; see also Table 2). Additionally, soil moisture measurements are also missing for Sion (32%). As the data gaps in both data series mostly do not overlap, the overall number of available data in Sion is very low. This does not fully apply to the comparison between SWI and SMI in Sion though, as the SMI data series is continuously available for the whole analyzed time period (see also Table 2). Overall, the missing data gaps are thus much shorter.

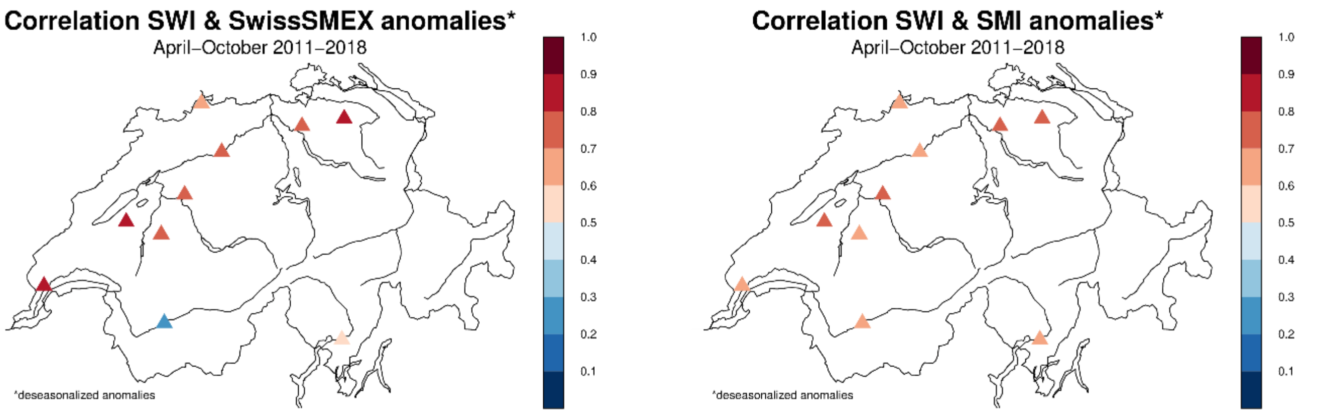

(**a**) (**b**)

Figure 5. Correlations of (**a**) the ASCAT soil water index (SWI) and the SwissSMEX soil moisture measurements and (**b**) the SWI and the soil moisture index (SMI) at the ten considered grassland sites during April to October from 2011 to 2018 based on deseasonalized anomalies.

In terms of evapotranspiration, the dry years are visible in the measured evapotranspiration data from the lysimeter at the grassland site in Rietholzbach (Figure 6a). In contrast to the observed low soil moisture levels in 2015 and 2018, the dry years stand out with mostly above-average amounts of evapotranspiration in the summer, especially in 2015. This is also the case for 2003 as one of the driest years in the last decade [42] and it is included here in addition. The high rate of evapotranspiration in dry conditions indicates that the exchange of water vapor with the atmosphere is mainly driven by available energy, while soil water is still abundantly accessible for evaporation and plant transpiration at the surface at this humid site. Only in July 2003 and June 2015 is there an observable substantial decrease in summer ET relative to the long-term mean climatology, which at least in the case of 2015 is the result of humid atmospheric conditions rather than soil water limitation. In addition, downhill lateral water flow, topographic shadowing, and water-saving forests around the grassland site might contribute to sustained high evapotranspiration rates during the dry periods. Rietholzbach, in turn, is the only measurement site in Switzerland, where long-term and high-quality in situ evapotranspiration data are available.

The climatologies (based on the 2006–2014 time period) of the satellite-based data agree well with the in situ measurements at the Rietholzbach site (Figure 6b). The anomaly correlation between the in situ measurements and ET is 0.67 (with a mean bias of the absolute values of -0.12 mm), while it is lower for ETP with $r = 0.63$ (and a mean bias of the absolute values of 0.27 mm). The lower correlation is mainly due to the influence of snow cover during the winter months (see further below). The influence of the snow cover is also reflected in the lower NSE and higher RMSE between the in situ measurements and ETP. The NSE and RMSE between the in situ measurements and ET are 0.73 and 0.84 mm, which are close to the maximum RMSE reported by [35] for ETo (0.7 mm). In the case of ETP, the NSE and RMSE are 0.52 and 1.14 mm. For the period of April–October both time series ET and ETP are consistent with the measured data, with ETP being slightly closer to the in situ reference. The minor underestimation of actual evapotranspiration during the summer half-year may thereby result from a marginal overestimation of soil water limitation at the Rietholzbach site in the ET algorithm. However, the overall small discrepancy between ET and ETP indicates that the high water availability at this location, as reported above, is reasonably captured in the algorithm. During November–March, when there can be snow cover, ETP is clearly higher than ET, i.e., the liquid water availability is substantially diminished.

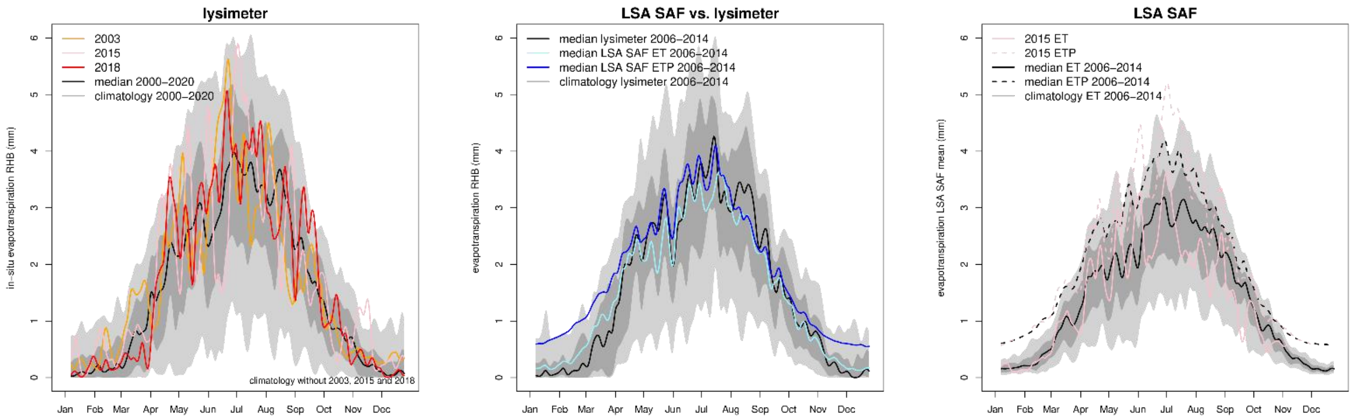

(**a**) (**b**) (**c**)

Figure 6. Seasonal evolution of daily evapotranspiration from (**a**) long-term lysimeter measurements at the Rietholzbach site from 2000 to 2020, (**b**) lysimeter measurements and satellite-based data at the Rietholzbach site from 2006 to 2014, and (**c**) spatially-aggregated satellite-based data from 2006 to 2014 (based on the grid cells closest to the ten considered grassland stations). The dark grey shading shows the 25–75% range of the respective background climatology; the light grey shading shows the 5–95% range. The evolution of the respective median as well as of the covered dry years is highlighted.

The representation of spatially heterogeneous water availability in the satellite-based data series at the considered ten grassland sites is demonstrated in Figure 6c. The medians of spatially-aggregated satellite-based ET and ETP for the entire period as well as for 2015 differ considerably throughout the seasonal cycle. This difference is by large a result of three stations out of ten, where the actual evapotranspiration rate is substantially smaller than the corresponding potential rate: Basel, Sion, and Cadenazzo (see Figure 7a,b). All three locations can be climatologically characterized as rather dry and warm. Hence, we consider it plausible that the modelled ET is significantly influenced by water limitations at these locations. Unfortunately, we lack the in situ measurements to test this outcome with statistical confidence.

Figure 6c shows the dry year of 2015 in contrast to the seasonal pattern of evapotranspiration across all of the considered sites. It becomes apparent that the precipitation deficit in summer 2015 is reflected in a smaller ET on average, while the high available energy in 2015 results in higher ETP. The response of the satellite-based model to drought thus seems adequate.

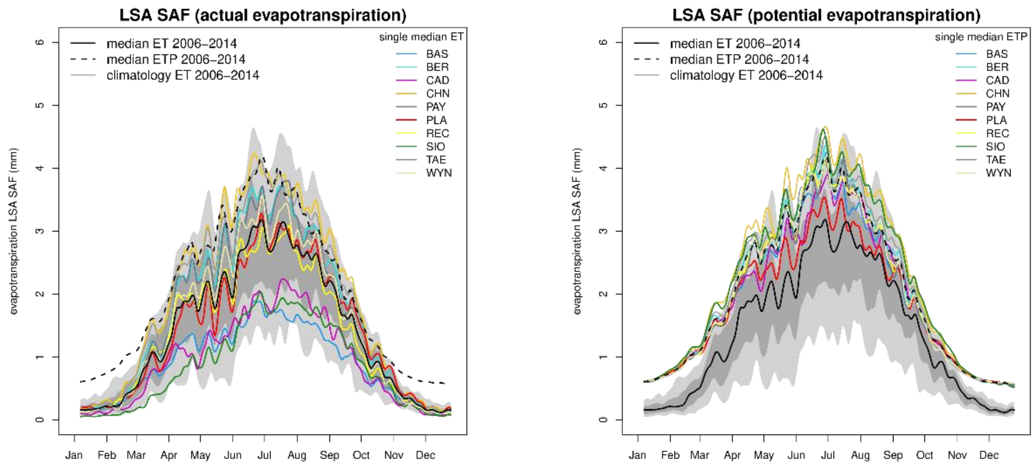

(**a**) (**b**)

Figure 7. Seasonal evolution of daily evapotranspiration from spatially-aggregated satellite-based data from 2006 to 2014 (based on the grid cells closest to the ten considered grassland stations). The dark grey shading shows the 25–75% range; the light grey shading shows the 5–95% range. The median of the respective time series as well as the evolution of the (**a**) single actual evapotranspiration (ET) median and (**b**) the single potential evapotranspiration (ETP) median for each station is highlighted.

4. Discussion

This study demonstrates the high potential of EUMETSAT SAF satellite data to complement station-based drought monitoring with spatial information in the orographically challenging region of Switzerland. Several different drought parameters were considered, which allows for a multivariate perspective on droughts. All considered datasets were thoroughly validated in the previous studies.

More precisely, the study included satellite-based land surface temperature, vegetation, soil moisture and potential, and actual evapotranspiration data, which were transferred to climatological drought indices. These spatial datasets were compared with the standardized precipitation index (SPI), both measured and modelled soil moisture data, and with evapotranspiration measurements at ten different grassland sites in Switzerland. For the evapotranspiration analysis, another grassland site (Rietholzbach) was included due to its continuous and high-quality data coverage. The results find clear signals associated with drought conditions in all of the analyzed indices. The major drought events of 2003, 2015, and 2018 are well represented.

More precisely, soil water shortage was well visible in the ASCAT soil water index (SWI) data from the H SAF network for the analyzed drought events in Switzerland. The comparison of in situ and modelled soil moisture data with the satellite-based data shows strong agreement in terms of anomalies. SWI indicates high anomaly correlations of 0.56 to 0.83 (except Sion) with in situ measurements. SWI also correlates high (0.63 to 0.76) with the model-based SMI data. These correlations are higher compared to other studies [32]. None of the investigated stations is situated directly in the mountains. Hence, those results are valid for Northern and Southern Switzerland, where a major drought with a significant socio-economic impact appeared in the last few years. It also needs to be noted that the ASCAT SWI has a poor performance over snow [33,44], which was not evaluated in this study.

For all three drought events in Switzerland, anomalously high land surface temperatures (LSTs) could be observed. In 2018, the temperature anomaly was particularly pronounced. CM SAF LSTs now cover the entire WMO climatological norm period of 1991–2020 and can thus well characterize droughts in a changing climate. Combined with the satellite-based vegetation condition index (VCI), LST climate data allow for mapping and visualizing drought as the vegetation health index (VHI) for long time periods of 30 years+. Satellite-based LST products are clear sky products [56]. For periods with persistent cloud coverage, which is often not the case during drought events, gaps in weekly VHI products can appear and hence limit its use for operational monitoring.

Finally, the analysis of short-term LSA SAF evapotranspiration data in this study demonstrates that evapotranspiration anomalies can be well characterized using satellite data. In particular, the year 2015 showed a clear signal of dry conditions. The Meteosat evapotranspiration datasets agreed well with the measurements in terms of deseasonalized anomalies, with correlations of 0.63 and 0.67 for potential and actual evapotranspiration, respectively. The actual evapotranspiration offers a slightly higher agreement, precisely because it is not so overrated in the wintertime. Monitoring drought events through evapotranspiration is, however, not as straightforward as for the remaining drought indicators. It strongly depends on the location and the local soil water availability whether evapotranspiration increases or decreases during dry and hot conditions (energy-limited vs. soil water-limited regime). The humid site in Rietholzbach showed mostly an excess in measured evapotranspiration during dry periods, which can significantly contribute to the soil water deficit (e.g., [42]). With drier climate conditions and during strong droughts, the amplifying role of evapotranspiration will however reduce, and soil moisture can become limiting, a condition that was observed in August 2003 at the Rietholzbach site [42]. In terms of evaluating the LSA SAF ET products for their ability to monitor droughts in different regions in Switzerland and different hydrological conditions with in situ data, this study and the findings in this regard are limited by the fact that only one station is available.

Overall, the results of this study show the high potential of satellite-based data from the EUMETSAT SAF network for operational drought monitoring systems, especially when using a combination of different drought indicators. When aiming for impact-based and holistic drought monitoring, we thus suggest the following:

- As drought is a complex phenomenon and different parts of natural systems are affected at different time scales, we argue with using a combination of different drought indicators within a drought monitoring system.
- Soil moisture is a fundamental component when it comes to effective drought monitoring. As soil water deficit can be observed at the onset of a drought event, depicting its anomalies is especially effective for drought monitoring and early warning provisions in Switzerland.
- In addition, the land surface temperature (LST) and vegetation health are important components of an effective drought monitoring system. They help to evaluate the impacts of drought on natural vegetation during the growing season. The VHI monitors drought at a relatively advanced stadium, after negative soil moisture anomalies are visible and water stress is shown in the vegetation cover.
- In light of the projected increase in summer drying in Switzerland [7], and overall in Central and Western Europe [8], we consider it essential to have information on evapotranspiration included in the drought monitoring system. Satellite-based actual evapotranspiration will be released as 30 years+ CM SAF climate data records in 2022.
- When setting up ground validation sites for comparison with remote sensing datasets, care should be taken that the station set offers a high spatial variability. Wet and dry locations should be available to analyze the above-mentioned processes and their influence on the performance of the satellite data. This holds true for all of the considered indicators.
- Future analyses with focus on the concrete integration of satellite- and ground-based drought information which is needed to generate a comprehensive climatological drought monitoring system for Switzerland.

Although this work is devoted to drought monitoring in Switzerland, it could provide support in the revision process of any drought monitoring system and it paves the way for further reassessments of climatological drought monitoring using satellite data.

Author Contributions: Conceptualization, A.R., A.D.-T., D.M. and M.H.; methodology, A.R., A.D.-T., D.M. and M.H.; formal analysis, A.R., D.M. and M.H.; writing—original draft preparation, A.R., D.M. and M.H.; writing—review and editing, A.D.-T., D.M., M.H. and S.I.S.; visualization, A.R., D.M. and M.H.; supervision, A.D.-T. and S.I.S. All authors have read and agreed to the published version of the manuscript.

Funding: A.B. and A.D.T. thank the Federal Office of Meteorology and Climatology MeteoSwiss, who made it possible to carry out this study. D.M., M.H. and S.I.S. acknowledge financial support from GCOS Switzerland through the SMiLE-ECV-CH project.

Institutional Review Board Statement: Not applicable.

Informed Consent Statement: Not applicable.

Data Availability Statement: The SAF data on land surface temperature and potential evapotranspiration are publicly available via the EUMETSAT Drought & Vegetation Data Cube (https://training.eumetsat.int/course/view.php?id=399 accessed on 22 November 2022). The SwissSMEX soil moisture and evapotranspiration measurements are available upon request (https://iac.ethz.ch/group/land-climate-dynamics/research/swisssmex.html accessed on 22 November 2022).

Acknowledgments: The work performed was completed, i.a., by using data from EUMETSAT's Satellite Application Facilities on Climate Monitoring (CM SAF), data in Support to Operational Hydrology and Water Management (H SAF) and Land Surface Analysis (LSA SAF). The ASCAT SWI data set was developed within the BMon project (ASAP Project No. 872408 funded by the Austrian Research Promotion Agency (FFG). We would like to thank all data providers and MeteoSwiss for allowing us to carry out the work within the framework of this evaluation study. D.M., M.H. and S.I.S. acknowledge GCOS Switzerland for partial funding through the SMiLE-ECV-CH project.

Conflicts of Interest: The authors declare no conflict of interest. The funders had no role in the design of the study; in the collection, analyses, or interpretation of data; in the writing of the manuscript; or in the decision to publish the results.

References

1. Burton, I.; Kates, R.W.; White, G.F. *The Environment as Hazard*; Oxford University Press: Oxford, UK, 1978; p. 240.
2. World Meteorological Organization (WMO); Global Water Partnership (GWP). National Drought Management Policy Guidelines: A Template for Action. 2014. Available online: https://www.droughtmanagement.info/literature/IDMP_NDMPG_en.pdf (accessed on 14 October 2021).
3. FOEN. *Hitze und Trockenheit im Sommer 2015. Auswirkungen auf Mensch und Umwelt*; Umwelt-Zustand. Bundesamt für Umwelt BAFU: Bern, Switzerland, 2016; Volume 1629, p. 108.
4. MeteoSwiss. Hitze und Trockenheit im Sommerhalbjahr 2018–eine klimatologische Übersicht. *Fachber. MeteoSchweiz* **2018**, *272*, 38.
5. FOEN. *Hitze und Trockenheit im Sommer 2018. Auswirkungen auf Mensch und Umwelt*; Umwelt-Zustand. Bundesamt für Umwelt: Bern, Switzerland, 2019; Volume 1909, p. 91.
6. Blauhut, V.; Stoelzle, M.; Ahopelto, L.; Brunner, M.I.; Teutschbein, C.; Wendt, D.E.; Akstinas, V.; Bakke, S.J.; Barker, L.J.; Bartošová, L.; et al. Lessons from the 2018–2019 European droughts: A collective need for unifying drought risk management. *Nat. Hazards Earth Syst. Sci. Discuss* **2021**, *22*, 2201–2217. [CrossRef]
7. CH2018. CH2018—Climate Scenarios for Switzerland, National Centre for Climate Services. 2018. Available online: https://www.nccs.admin.ch/nccs/de/home/klimawandel-und-auswirkungen/schweizer-klimaszenarien.html (accessed on 14 October 2021).
8. Seneviratne, S.I.; Zhang, X.; Adnan, M.; Badi, W.; Dereczynski, C.; Di Luca, A.; Ghosh, S.; Iskandar, I.; Kossin, J.; Lewis, S.; et al. Weather and Climate Extreme Events in a Changing Climate. In *Climate Change 2021: The Physical Science Basis. Contribution of Working Group I to the Sixth Assessment Report of the Intergovernmental Panel on Climate Change*; Masson-Delmotte, V., Zhai, P., Pirani, A., Connors, S.L., Péan, C., Berger, S., Caud, N., Chen, Y., Goldfarb, L., Gomis, M.I., et al., Eds.; Cambridge University Press: Cambridge, UK; New York, NY, USA, 2021; pp. 1513–1766.
9. McKee, T.B.; Doesken, N.J.; Kleist, J. The relationship of drought frequency and duration to time scales. *Eighth Conf. Appl. Climatol.* **1993**, *17*, 179–183.
10. Vicente-Serrano, S.M.; Beguería, S.; López-Moreno, J.I. A multiscalar drought index sensitive to global warming: The standardized precipitation evapotranspiration index. *J. Clim.* **2010**, *23*, 1696–1718. [CrossRef]
11. Brown, J.F.; Reed, B.C.; Hayes, M.J.; Wilhite, D.A.; Hubbard, K. A prototype drought monitoring system integrating climate and satellite data. In Proceedings of the 15th William T. Pecora Memorial Symposium on Remote Sensing, Denver, CO, USA, 10–15 November 2002; pp. 1–11.

12. Enenkel, E.; Steiner, C.; Mistelbauer, T.; Dorigo, W.; Wagner, W.; See, L.; Atzberger, C.; Schneider, S.; Rogenhofer, E. A combined satellite-derived Drought Indicator to support Humanitarian Aid Organizations. *Remote Sens.* **2016**, *8*, 340. [CrossRef]
13. Hao, Z.; AghaKouchak, A. multivariate standardized drought index: A parametric multi-index model. *Adv. Water Resour.* **2013**, *57*, 12–18. [CrossRef]
14. Hao, Z.; Singh, V.P. Drought characterization from a multivariate perspective: A review. *J. Hydrol.* **2015**, *527*, 668–678. [CrossRef]
15. Lloyd-Hughes, B.; Saunders, M.A. A drought climatology for Europe. *Int. J. Climatol.* **2002**, *22*, 1571–1592. [CrossRef]
16. Hillel, D. *Environmental Soil Physics*; Academic Press: San Diego, CA, USA, 1998; p. 771.
17. Seneviratne, S.I.; Corti, T.; Davin, E.L.; Hirschi, M.; Jaeger, E.B.; Lehner, I.; Orlowsky, B.; Teuling, A.J. Investigating soil moisture-climate interactions in a changing climate: A review. *Earth-Sci. Rev.* **2010**, *99*, 125–161. [CrossRef]
18. AghaKouchak, A.; Farahmand, A.; Melton, F.S.; Teixeira, J.; Anderson, M.C.; Wardlow, B.D.; Hain, C.R. Remote sensing of drought: Progress, challenges and opportunities. *Rev. Geophys.* **2015**, *53*, 452–480. [CrossRef]
19. Ford, T.W.; Quiring, S.M. Comparison of contemporary in situ, model, and satellite remote sensing soil moisture with a focus on drought monitoring. *Water Resour. Res.* **2019**, *55*, 1565–1582. [CrossRef]
20. UN. Data Application of the Month: Drought Monitoring. 2021. Available online: https://www.un-spider.org/links-and-resources/data-sources/daotm-drought (accessed on 15 October 2021).
21. Gutman, G.G. Towards monitoring droughts from space. *J. Clim.* **1990**, *3*, 282–295. [CrossRef]
22. Singh, R. P.; Roy, S.; Kogan, F. Vegetation and temperature condition indices from NOAA AVHRR data for drought monitoring over India. *Int. J. Remote Sens.* **2003**, *24*, 4393–4402. [CrossRef]
23. Seiler, R.; Kogan, F.; Sullivan, J. AVHRR-based vegetation and temperature condition indices for drought detection in Argentina. *Adv. Space Res.* **1998**, *213*, 481–484. [CrossRef]
24. Kogan, F.N. Operational space technology for global vegetation assessment. *Bull. Am. Meteorol. Soc.* **2001**, *82*, 1949–1964. [CrossRef]
25. Chang, S.; Chen, H.; Wu, B.; Nasanbat, E.; Yan, N.; Davdai, B. A practical satellite-derived vegetation drought index for arid and semi-arid grassland drought monitoring. *Remote Sens.* **2021**, *13*, 414. [CrossRef]
26. Steele-Dunne, S.C.; Hahn, S.; Wagner, W.; Vreugdenhil, M. Towards including dynamic vegetation parameters in the EUMETSAT H SAF ASCAT soil moisture products. *Remote Sens.* **2021**, *13*, 1463. [CrossRef]
27. Orimoloye, I.R. Agricultural drought and its potential impacts: Enabling decision-support for food security in vulnerable regions. *Front. Sustain. Food Syst.* **2022**, *6*, 838824. [CrossRef]
28. Hirschi, M.; Davin, E.L.; Schwingshackl, C.; Wartenburger, R.; Meier, R.; Gudmundsson, L.; Seneviratne, S.I. *Soil Moisture and Evapotranspiration. Hydro-CH2018 Project*; Commissioned by the Federal Office for the Environment (FOEN): Bern, Switzerland, 2020; p. 48.
29. FOEN. Effects of climate change on Swiss water bodies. Hydrology, water ecology and water management. *Environ. Stud.* **2021**, *210*, 125.
30. Manesh, M.B.; Khosravi, H.; Alamdarloo, E.H.; Alekasir, M.S.; Gholami, A.; Singh, V.P. Linkage of agricultural drought with meteorological drought in different climates of Iran. *Theor. Appl. Climatol.* **2019**, *138*, 1025–1033. [CrossRef]
31. Kogan, F.N. Application of vegetation index and brightness temperature for drought detection. *Adv. Space Res.* **1995**, *15*, 91–100. [CrossRef]
32. Bauer-Marschallinger, B. *Copernicus Global Land Operation "Vegetation and Energy"*; Product User Manual; Copernicus Global Land Operations: Prague, Czech Republic, 2018; p. 51.
33. Hahn, S. Product User Manual (PUM) Surface Soil Moisture ASCAT NRT Orbit. 2016, p. 20. Available online: SAF/HSAF/CDOP2/PUM-SSM_ASCAT_NRT_O (accessed on 12 July 2021).
34. CM SAF Project Team. Product User Manual Land Surface Temperature (LST). 2017, p. 24. Available online: www.cmsaf.eu (accessed on 18 July 2022).
35. LSA SAF Project Team (IPMA). Product User Manual Reference Evapotranspiration (DMETREF). 2016, p. 25. Available online: SAF/LAND/IPMA/PUM_ETREF/1.1 (accessed on 13 October 2021).
36. LSA SAF Project Team (RMI). Product User Manual for Evapotranspiration and Surface Fluxes (ET & SF v2). 2018, p. 35. Available online: SAF/LAND/RMI/VR/1.1 (accessed on 12 June 2021).
37. Gouveia, C.M.; Martins, J.P.A.; Russo, A.; Durão, R.; Trigo, I.F. Monitoring Heat Extremes across Central Europe Using Land Surface Temperature Data Records from SEVIRI/MSG. *Remote Sens.* **2022**, *14*, 3470. [CrossRef]
38. Feldman, A.F.; Gianotti, D.J.S.; Trigo, I.F.; Salvucci, G.D.; Entekhabi, D. Land-atmosphere drivers of landscape-scale plant water content loss. *Geophys. Res. Lett.* **2020**, *47*, e2020GL090331. [CrossRef]
39. Tagesson, T.; Horion, S.; Nieto, H.; Fornies, V.Z.; González, G.M.; Bulgin, C.E.; Fensholt, R. Disaggregation of SMOS soil moisture over West Africa using the Temperature and Vegetation Dryness Index based on SEVIRI land surface parameters. *Remote Sens. Environ.* **2018**, *206*, 424–441. [CrossRef]
40. Scherrer, S.C.; Hirschi, M.; Spirig, C.; Maurer, F.; Kotlarski, S. Trends and drivers of recent summer drying in Switzerland. *Environ. Res. Commun.* **2022**, *4*, 025004. [CrossRef]
41. Mittelbach, H.; Seneviratne, S.I. A new perspective on the spatio-temporal variability of soil moisture: Temporal dynamics versus time-invariant contributions. *Hydrol. Earth Syst. Sci.* **2012**, *16*, 2169–2179. [CrossRef]

42. Seneviratne, S.I.; Lehner, I.; Gurtz, J.; Teuling, A.J.; Lang, H.; Moser, U.; Grebner, D.; Menzel, L.; Schroff, K.; Vitvar, T.; et al. Swiss prealpine Rietholzbach research catchment and lysimeter: 32 year time series and 2003 drought event. *Water Resour. Res.* **2012**, *48*, 20. [CrossRef]
43. Hirschi, M.; Michel, D.; Lehner, I.; Seneviratne, S.I. A site-level comparison of lysimeter and eddy covariance flux measurements of evapotranspiration. *Hydrol. Earth Syst. Sci.* **2017**, *21*, 1809–1825. [CrossRef]
44. Bartalis, Z.; Naeimi, V.; Hasenauer, S.; Wagner, W. ASCAT Soil Moisture Product Handbook. In *ASCAT Soil Moisture Report Series*; Institute of Photogrammetry and Remote Sensing, Vienna University of Technology: Vienna, Austria, 2008; Volume 15.
45. Wagner, W.; Lemoine, G.; Rott, H. A method for estimating soil moisture from ERS scatterometer and soil data. *Remote Sens. Environ.* **1999**, *70*, 191–207. [CrossRef]
46. Ceballos, A.; Scipal, K.; Wagner, W.; Martínez-Fernández, J. Validation of ERS scatterometer-derived soil moisture data over the central part of the Duero Basin, Spain. *Hydrol. Process.* **2005**, *19*, 1549–1566. [CrossRef]
47. Albergel, C.; Rüdiger, C.; Pellarin, T.; Calvet, J.-C.; Fritz, N.; Froissard, F.; Suquia, D.; Petitpa, A.; Piguet, B.; Martin, E. From near-surface to root-zone soil moisture using an exponential filter: An assessment of the method based on in-situ observations and model simulations. *Hydrol. Earth Syst. Sci.* **2008**, *12*, 1323–1337. [CrossRef]
48. Tong, R.; Parajka, J.; Salentinig, A.; Pfeil, I.; Komma, J.; Széles, B.; Kubán, M.; Valent, P.; Vreugdenhil, M.; Wagner, W.; et al. The value of ASCAT soil moisture and MODIS snow cover data for calibrating a conceptual hydrologic model. *Hydrol. Earth Syst. Sci.* **2021**, *25*, 1389–1410. [CrossRef]
49. Parajka, J.; Naeimi, V.; Blöschl, G.; Wagner, W.; Merz, R.; Scipal, K. Assimilating scatterometer soil moisture data into conceptual hydrologic models at the regional scale. *Hydrol. Earth Syst. Sci.* **2006**, *10*, 353–368. [CrossRef]
50. Duguay-Tetzlaff, A.; Bento, V.A.; Göttsche, F.M.; Stöckli, R.; Martins, J.P.A.; Trigo, I.; Olesen, F.; Bojanowski, J.S.; Da Camara, C.; Kunz, H. Meteosat Land Surface Temperature Climate Data Record. Achievable Accuracy and Potential Uncertainties. *Remote Sens.* **2015**, *7*, 13139–13156. [CrossRef]
51. Bento, V.A.; Trigo, I.F.; Gouveia, C.M.; DaCamara, C.C. Contribution of Land Surface Temperature (TCI) to Vegetation Health Index: A Comparative Study Using Clear Sky and All-Weather Climate Data Records. *Remote Sens.* **2018**, *10*, 1324. [CrossRef]
52. Hupet, F.; Bogaert, P.; Vanclooster, M. Quantifying the local-scale uncertainty of estimated actual evapotranspiration. *Hydrol. Process.* **2004**, *18*, 3415–3434. [CrossRef]
53. Ruth, C.E.; Michel, D.; Hirschi, M.; Seneviratne, S.I. Comparative study of a long-established large weighing lysimeter and a state-of-the-art mini-lysimeter. *Vadose Zone J.* **2018**, *17*, 1–10. [CrossRef]
54. World Meteorological Organization (WMO); Global Water Partnership (GWP). *Handbook of Drought Indicators and Indices (M. Svoboda and B.A. Fuchs)*; Integrated Drought Management Programme (IDMP), Integrated Drought Management Tools and Guidelines Series 2; WMO: Geneva, Switzerland, 2016; Available online: https://www.droughtmanagement.info/literature/GWP_Handbook_of_Drought_Indicators_and_Indices_2016.pdf (accessed on 6 September 2022).
55. Woli, P.; Jones, J.W.; Ingram, K.T.; Fraisse, C.W. Agricultural Reference Index for Drought (ARID). *Agron. J.* **2012**, *104*, 287–300. [CrossRef]
56. Paulik, C.; Dorigo, W.; Wagner, W.; Kidd, R. Validation of the ASCAT Soil Water Index using in situ data from the International Soil Moisture Network. *Int. J. Appl. Earth Obs. Geoinf.* **2014**, *30*, 1–8. [CrossRef]